



**Universidade de São Paulo**

**Biblioteca Digital da Produção Intelectual - BDPI**

---

Departamento de Física e Ciências Materiais - IFSC/FCM

Artigos e Materiais de Revistas Científicas - IFSC/FCM

---

2009-10

# Penicillin biosensor based on a capacitive field-effect structure functionalized with a dendrimer/carbon nanotube multilayer

---

Biosensors and Bioelectronics, Oxford, v. 25, n. 2, p. 497-501, Oct. 2009

<http://www.producao.usp.br/handle/BDPI/49375>

*Downloaded from: Biblioteca Digital da Produção Intelectual - BDPI, Universidade de São Paulo*



Short communication

## Penicillin biosensor based on a capacitive field-effect structure functionalized with a dendrimer/carbon nanotube multilayer

José R. Siqueira Jr.<sup>a,b,c</sup>, Maryam H. Abouzar<sup>b,c</sup>, Arshak Poghossian<sup>b,c</sup>, Valtencir Zucolotto<sup>a</sup>, Osvaldo N. Oliveira Jr.<sup>a,\*</sup>, Michael J. Schöning<sup>b,c,\*\*</sup>

<sup>a</sup> Instituto de Física de São Carlos, USP, CP 369, 13560-970 São Carlos, Brazil

<sup>b</sup> Institute of Nano- and Biotechnologies, Aachen University of Applied Sciences, 52428 Jülich, Germany

<sup>c</sup> Institute of Bio- and Nanosystems (IBN2), Research Centre Jülich, 52425 Jülich, Germany

## ARTICLE INFO

## Article history:

Received 6 May 2009

Received in revised form 23 June 2009

Accepted 13 July 2009

Available online 16 July 2009

## Keywords:

Capacitive

electrolyte-insulator-semiconductor sensor

Field-effect devices

Penicillin biosensor

Layer-by-layer

Carbon nanotubes

Dendrimers

## ABSTRACT

Silicon-based sensors incorporating biomolecules are advantageous for processing and possible biological recognition in a small, reliable and rugged manufactured device. In this study, we report on the functionalization of field-effect (bio-)chemical sensors with layer-by-layer (LbL) films containing single-walled carbon nanotubes (SWNTs) and polyamidoamine (PAMAM) dendrimers. A capacitive electrolyte-insulator-semiconductor (EIS) structure modified with carbon nanotubes (EIS-NT) was built, which could be used as a penicillin biosensor. From atomic force microscopy (AFM) and field-emission scanning electron microscopy (FESEM) images, the LbL films were shown to be highly porous due to interpenetration of SWNTs into the dendrimer layers. Capacitance–voltage ( $C/V$ ) measurements pointed to a high pH sensitivity of ca. 55 mV/pH for the EIS-NT structures. The biosensing ability towards penicillin of an EIS-NT-penicillinase biosensor was also observed as the flat-band voltage shifted to lower potentials at different penicillin concentrations. A dynamic response of penicillin concentrations, ranging from 5.0  $\mu\text{M}$  to 25 mM, was evaluated for an EIS-NT with the penicillinase enzyme immobilized onto the surfaces, via constant–capacitance (ConCap) measurements, achieving a sensitivity of ca. 116 mV/decade. The presence of the nanostructured PAMAM/SWNT LbL film led to sensors with higher sensitivity and better performance.

© 2009 Elsevier B.V. All rights reserved.

### 1. Introduction

Research in (bio-)chemical sensors is inherently multidisciplinary, especially when different technologies are integrated into single devices for various technological applications (Patolsky et al., 2007; Lutkenhaus and Hammond, 2007). This is the case for silicon-based (bio-)chemical sensors, which exhibit advantages in terms of processing and possibility of achieving biological recognition in small, reliable and rugged manufactured devices. These sensors may be applied in medicine and biotechnological processes, as well as in food control and environmental monitoring (Schöning and Poghossian, 2006, 2008; Abouzar et al., 2008; Poghossian et al., 2006, 2007a,b; Gun et al., 2008). Efforts in this field have been devoted to the miniaturization and integration of sensors, actuators

and mechanical or fluidic elements into a single chip (Patolsky et al., 2007; Schöning and Poghossian, 2008).

The introduction of an additional ion- and/or charge-sensitive gate layer into (bio-)chemical field-effect devices (FEDs) makes them sensitive to any electrical or electrochemical interaction at or nearby the interface to the electrolyte. The simplest (bio-)chemical FED is the capacitive electrolyte-insulator-semiconductor (EIS) structure that represents a (bio-)chemically sensitive capacitor. The operation principle is based on changes in the electrical surface charge of the EIS structure, which modulate its capacitance. The use of EIS sensors is attractive from a commercial point of view due to their low-cost of processing (usually no photolithographic or complicated encapsulation process steps are required) and miniaturized size (Schöning and Poghossian, 2006, 2008; Abouzar et al., 2008; Poghossian et al., 2007a,b; Gun et al., 2008; Siqueira et al., 2009).

The development of new methods and implementation of novel materials for desirable biocomposite nanostructures has been the subject of intensive research. Carbon nanotubes (CNTs) are attractive for (bio-)chemical sensors because of their unique properties, which in most cases arise from the combination of electrical and chemical properties and nanosized dimensions (Balasubramanian

\* Corresponding author at: Instituto de Física de São Carlos, USP, CP 369, 13560-970 São Carlos, Brazil Tel.: +55 16 3373 9825.

\*\* Corresponding author at: Institute of Nano- and Biotechnologies, Aachen University of Applied Sciences, 52428 Jülich, Germany Tel.: +49 0241 6009 53215.

E-mail addresses: [chu@ifsc.usp.br](mailto:chu@ifsc.usp.br) (O.N. Oliveira Jr.), [m.j.schoening@fz-juelich.de](mailto:m.j.schoening@fz-juelich.de) (M.J. Schöning).

and Burghard, 2006; Kim et al., 2007; Allen et al., 2007; Byon and Choi, 2006). One simple, versatile method to assemble dispersed CNTs is the layer-by-layer (LbL) technique, which offers fine control over film thickness and architecture (Hammond, 2004; Tang et al., 2006; Ariga et al., 2007), making it possible to combine different materials in a synergistic way (Jiang et al., 2004; Olek et al., 2004; Zucolotto et al., 2006; Siqueira et al., 2006, 2007; Xue et al., 2006; Zucolotto et al., 2007). As a building unit for the multilayer films in biosensors, CNTs have often been combined with polyelectrolytes and highly branched dendritic macromolecules (Yang et al., 2006; Siqueira et al., 2008; Siqueira et al., 2009).

Recently, we have described a new strategy for field-effect biosensing based on an EIS structure functionalized with an LbL multilayer of organic/inorganic nano-hybrids containing SWNTs and polyamidoamine (PAMAM) dendrimers (Siqueira et al., 2009). The generic approach was demonstrated with a penicillin biosensor using a capacitive EIS structure. In this paper, we extend the previous study with a detailed analysis of the sensitive characteristics for penicillin detection using a penicillin biosensor based on a capacitive EIS structure functionalized with a dendrimer/carbon nanotube multilayer. Furthermore, a discussion is made of the possible causes for the enhanced performance due to the incorporation of such nanostructure and of the advantages for further biosensing using the field-effect structures. The latter is accomplished by comparing results for three kinds of sensor: (i) obtained with immobilization of penicillinase onto the bare EIS sensor, (ii) EIS structures functionalized with PAMAM/PSS (poly(sodium 4-styrene sulfonate)) LbL films, and (iii) EIS structure functionalized with PAMAM/SWNT multilayers (EIS-NT).

## 2. Experimental

### 2.1. Materials and solutions

Fourth generation G4 PAMAM dendrimers, PSS with an average molecular weight (Mw) of ca. 70,000 and carboxylic acid functionalized SWNTs, prepared through the arc discharge technique, with 95% purity, length 0.5–1.5  $\mu\text{m}$ , and diameter of 1.5 and 3–5 nm for individual and bundled samples, respectively, were purchased from Sigma-Aldrich Co. The titrisol buffered solutions of PAMAM, PSS and SWNTs to produce LbL films were prepared with concentrations of 1.0  $\text{g L}^{-1}$ , at a pH 4 for the polyelectrolytes and pH 8 for the carbon nanotubes. The SWNT dispersion was obtained by adding 10 mg of the material in 10 mL of titrisol buffer solution under ultrasonication for 2 h, followed by filtration. In aqueous solution, the

carboxylic groups on the SWNT are deprotonated to carboxylate anions ( $\text{COO}^-$ ), yielding a negatively charged SWNT.

The enzyme penicillinase (*Bacillus cereus*, specific activity: 1670 units/mg protein) and penicillin G (benzyl penicillin, 1695 units/mg) were acquired from Sigma. The enzyme solution was prepared by dissolving penicillinase in a 0.2 M triethanolamine (TEA) buffer, pH 8. The penicillin solutions of different concentrations ranging from 5.0  $\mu\text{M}$  to 25 mM were prepared by dissolving penicillin G in a 0.5 mM polymix buffer, pH 8, containing 0.1 M KCl solution as an ionic strength adjuster.

### 2.2. Fabrication of EIS structures

The capacitive EIS structure of p-Si-SiO<sub>2</sub>-Ta<sub>2</sub>O<sub>5</sub> was prepared via thermal oxidation of Si in O<sub>2</sub> atmosphere at 1050 °C for 30 min to form a 30 nm SiO<sub>2</sub> insulating layer, while a 55 nm Ta<sub>2</sub>O<sub>5</sub> insulating, pH-sensitive layer was prepared via electron-beam evaporation of 30 nm Ta, followed by thermal oxidation at 515 °C during 30 min. A contact layer of Al film (300 nm) was deposited on the rear-side of the p-Si, and then the wafer was cut into single chips of 10 mm  $\times$  10 mm sizes. The EIS sensor was mounted into a homemade measuring cell and sealed by an O-ring to protect the side walls and backside contact of the chip from the electrolyte solution. The contact area of the EIS sensor with the solution was approximately 0.5 cm<sup>2</sup>.

### 2.3. LbL film preparation and enzyme immobilization

The multilayers of PAMAM/PSS and PAMAM/SWNT were obtained using the LbL assembly technique via consecutive dropping of respective PAMAM (for 5 min) and PSS (for 5 min) or PAMAM and SWNT (for 10 min) solutions into the cell, which was followed by rinsing and drying steps. These procedures were repeated until the desired number of bilayers was achieved. At the pH values of the solutions used, the surface of the Ta<sub>2</sub>O<sub>5</sub> layer was negatively charged by plasma treatment, and therefore we started formation of the LbL multilayers with the positively charged PAMAM.

The penicillin biosensor was completed after adsorptive immobilization of the enzyme penicillinase by dropping 80  $\mu\text{L}$  of its solution onto the Ta<sub>2</sub>O<sub>5</sub> substrate or the LbL film, with SWNT or PSS as outermost layer, and then dried at room temperature for 4 h. The sensor was subsequently rinsed thoroughly and stored in a polymix buffer pH 8 at 4 °C. The main advantages of the adsorptive immobilization are its simplicity and low cost with no loss of enzyme activity and the possibility of subsequent sensor

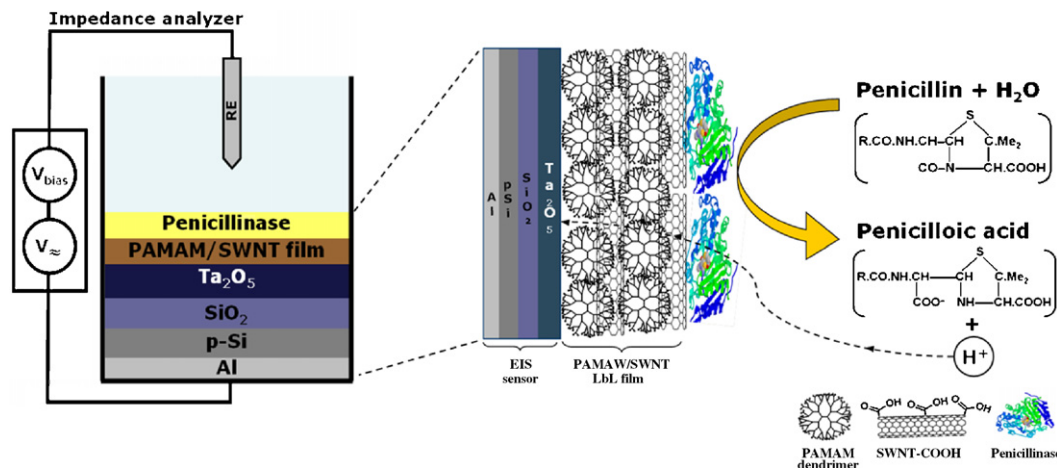


**Fig. 1.** Schematic representation of the structure, operation principle and chemical reaction of the penicillin biosensor based on an EIS structure functionalized with PAMAM/SWNT LbL film.

regeneration via repeated enzyme immobilization (Abouzar et al., 2008). Fig. 1 shows the schematic representation of the penicillin biosensor based on a capacitive EIS structure functionalized with a PAMAM/SWNT LbL film as well as the chemical structures of the materials employed.

#### 2.4. Physical and electrochemical characterization

The surface of the functionalized EIS sensors was analyzed with an atomic force microscope (AFM) BioMat Workstation (JPK Instruments, Germany) and a field-emission scanning electron microscopy (Gemini® FESEM Column LEO 1550 VP, Germany). Tapping mode liquid-cell AFM images were taken using Si cantilevers with silicon nitride tips. The scanned area was  $1.0 \mu\text{m} \times 1.0 \mu\text{m}$ . The morphology and root-mean-square (RMS) roughness of the PAMAM/PSS and PAMAM/SWNT multilayers were obtained from the height images.

The penicillin biosensors have been characterized by means of capacitance–voltage ( $C/V$ ) and constant–capacitance (ConCap) method at a frequency of 50 Hz using an impedance analyzer (Zahner Elektrik, Germany). The measuring setup is presented in Fig. 1. An ac voltage with an amplitude of 20 mV has been used for all measurements. In the ConCap mode, the capacitance of the EIS sensor is kept constant by using a feedback-control circuit that allows direct monitoring of potential changes at the sensor surface. A conventional liquid-junction Ag/AgCl electrode (Metrohm) was used as a reference electrode. The measurements have been performed in a dark Faraday cage at room temperature.

### 3. Results and discussion

#### 3.1. pH sensitivity of the EIS structures functionalized with the LbL films

Before enzyme immobilization and characterization of the penicillin biosensor, the pH sensitivity of the three proposed EIS sensors was investigated. This is required since the operation principle of a conventional capacitive EIS penicillin biosensor (without LbL film) is based on the detection of variations in the  $\text{H}^+$ -ion concentration due to the catalyzed hydrolysis of penicillin into penicilloic acid by the enzyme penicillinase (Abouzar et al., 2008; Siqueira et al., 2009). Fig. 2 shows the  $C/V$  curves (a) and the ConCap measurements for a three-bilayer EIS-NT sensor at pH ranging from 3 to 10. Taking as reference the pH sensitivity of a measured bare EIS structure with  $\text{Ta}_2\text{O}_5$  (ca. 57 mV/pH), the presence of the PAMAM/SWNT LbL film did not affect significantly the pH sensitivity of the EIS structure, which was ca. 55 mV/pH. This behavior may be explained by the high porosity of the LbL films formed by the interconnection of randomly oriented SWNT-networks into dendrimer layers, which allows the  $\text{H}^+$ -ions to penetrate through the film and reach the  $\text{Ta}_2\text{O}_5$  surface (see Fig. S1 in the supplementary material). Similar pH sensitivity was observed for the EIS-PAMAM/PSS sensor, but in this case it may be attributed to the low thickness of the polyelectrolyte film, which is ca. one tenth of the thickness of the PAMAM/SWNT films (ca. 32–35 nm) for the same number of bilayers. Moreover, ConCap measurements revealed that the functionalized EIS sensors exhibit a small drift, fast response time (ca. 10 s) and relatively low hysteresis (ca. 4 mV).

#### 3.2. Penicillin detection using EIS structures functionalized with the LbL films

The enzyme penicillinase was adsorbed onto the PAMAM/PSS and PAMAM/SWNT films and the biosensing ability towards penicillin G was investigated with  $C/V$  curves for an EIS-NT-penicillinase biosensor at different penicillin G concentrations from 0.25 mM to

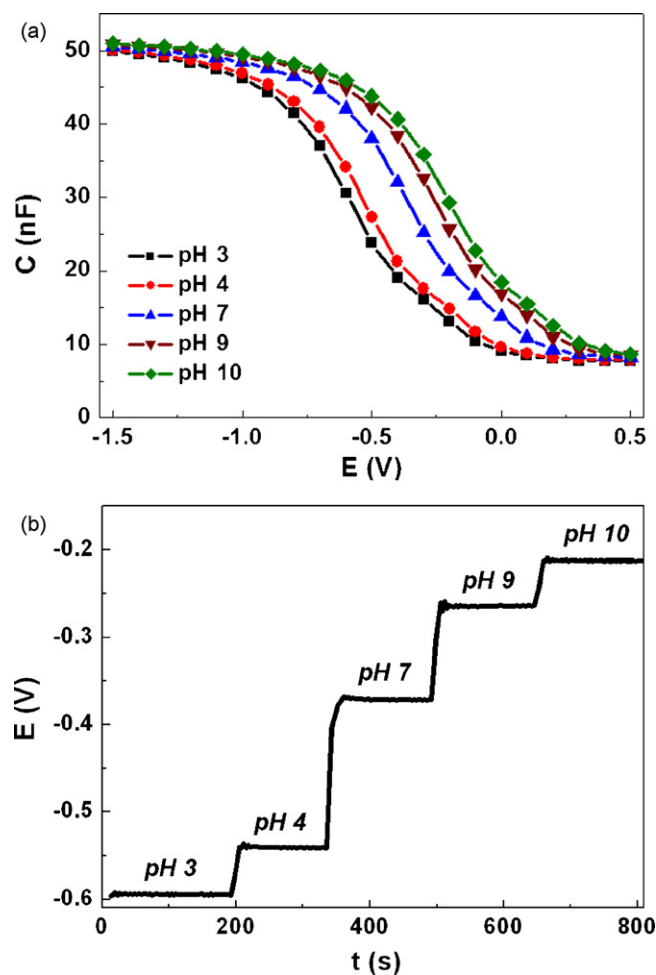
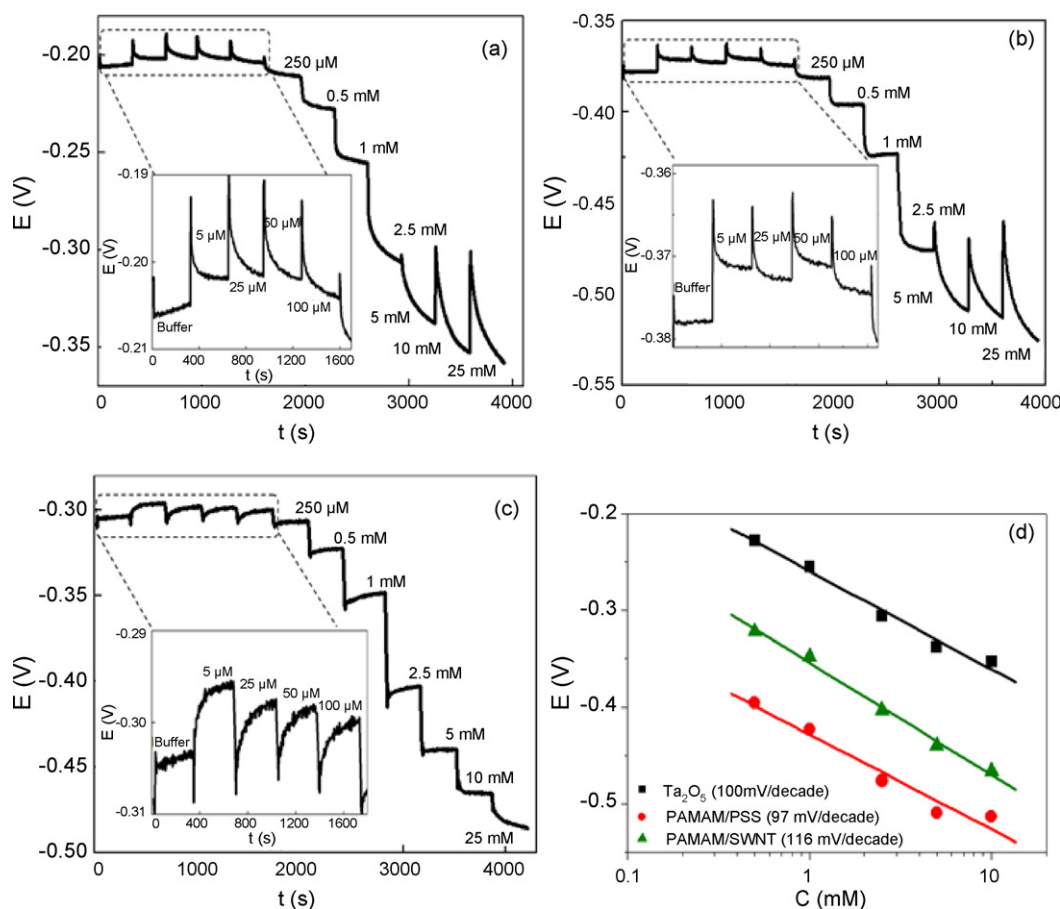


Fig. 2.  $C/V$  curves (a) and ConCap response (b) at different pH values for an EIS-NT sensor. Frequency: 50 Hz.

5.0 mM (see Fig. S2 in the supplementary material). The flat-band voltage shifted to lower values (zoomed area in the inset) with increasing penicillin G concentrations, which indicates an increased  $\text{H}^+$ -ion concentration at the sensor surface due to the enzymatic reaction. Note that this was also observed for bare EIS and EIS-PAMAM/PSS sensors.

In order to investigate in detail the difference on the sensitive characteristics of the functionalized EIS-penicillinase biosensors, they were further evaluated via ConCap measurements for a wider range of penicillin concentrations, from 5.0  $\mu\text{M}$  to 25 mM. Fig. 3 shows a ConCap dynamic response of penicillin concentrations for a bare EIS (a), EIS-PAMAM/PSS (b) and EIS-NT sensor (c), as well as their calibration curves (d). The increase in  $\text{H}^+$ -ion concentration from the enzymatic reaction in the presence of higher concentrated penicillin G solutions was determined from changes in the depletion potential at a working point of 32.5 nF. Both the bare EIS (with  $\text{Ta}_2\text{O}_5$  as pH-sensitive layer) and the EIS-PAMAM/PSS sensors showed a well defined sensitivity toward different penicillin concentrations.

The EIS-NT sensor displayed an even higher sensitivity and better performance. For a bare EIS sensor (Fig. 3a), the signal drift and the response time increased (to more than 5 min) after addition of 2.5 mM, while for the EIS-PAMAM/PSS sensor (Fig. 3b) the same occurred only after adding 10 mM. Moreover, the detection signal pointed to saturation above 10 mM for both sensors. In contrast, for an EIS-NT sensor (Fig. 3c), the response time remained constant (lower than 5 min) followed by a small signal drift up to



**Fig. 3.** ConCap response at different penicillin concentrations for a bare EIS (a), EIS-PAMAM/PSS (b), and EIS-NT sensor (c) and their respective calibration curves (d). Insets: zoom at low penicillin concentrations from 5 to 100  $\mu\text{M}$ .

a penicillin concentration of 25 mM. No saturation was observed for the concentration range analyzed. Such enhancement in the detection signal led to an increase in the linear concentration range. From 250  $\mu\text{M}$  to 25 mM, the sensitivity toward penicillin of the EIS-NT sensor was improved to 100 mV/decade, while in the same range the bare EIS and EIS-PAMAM/PSS sensors had 83 and 81 mV/decade, respectively. Considering the “best” linear range, viz. from 0.5 mM to 10 mM, the slope was 116 mV/decade for the EIS-NT sensor, while for the bare EIS and EIS-PAMAM/PSS sensor it was 100 and 98 mV/decade, respectively, as demonstrated in the calibration curve in Fig. 3d. Thus, the SWNT-LbL film on the EIS structure increased the sensitivity.

The influence from SWNTs on the sensors performance was also observed in the range of lowest concentrations (from 5  $\mu\text{M}$  to 100  $\mu\text{M}$ ), as depicted in the insets of Fig. 3a–c. At this concentration range, the potential was the same for the first three penicillin solutions. For the bare EIS and the EIS-PAMAM/PSS sensors, changes were only observed above 100  $\mu\text{M}$ , but for the EIS-NT sensor, a change in the potential was obtained upon addition of 25  $\mu\text{M}$  penicillin G, followed by further signal steps after addition of 50 and 100  $\mu\text{M}$ , respectively. Despite the small change in potential in this concentration range, the penicillin sensitivity was clearly improved in comparison to the other two EIS structures, indicating that SWNTs on the EIS sensor also cause an effect, which increases the penicillin sensitivity at low concentrations.

A comparison can also be made with similar work in the literature. (Abouzar et al., 2009) produced a penicillin biosensor based on an electrolyte-diamond-insulator-semiconductor (EDIS) sensor, which possessed a sensitivity of ca. 60–70 mV/decade, pH sensitivity of ca. 40 mV/pH and limit of detection around 5–25  $\mu\text{M}$ .

An amperometric and an EnFET penicillin biosensor reported by (Stred'anský et al., 2000) and (Lee et al., 2009) respectively, presented a limit of detection of ca. 10  $\mu\text{M}$ , with sensitivity of ca. 48 mV/mM and response time around 0.5–3 min. The EIS-NT-penicillin biosensor described here exhibited higher sensitivity and better stability with an improved response of the sensor signal. This is a consequence of the whole EIS-NT sensor structure ( $\text{p-Si-SiO}_2\text{-Ta}_2\text{O}_5\text{-(PAMAM/SWNT)}_3$ ).

The stability of the biosensor made with dendrimer/nanotubes is good as shown in Fig. 3c, where the drift of the sensor signal is practically null for various analyte concentrations. Such stability remained even for a period above 10 min. As for the long-term stability, we observed that the biosensors were still highly sensitive up to two weeks after fabrication. The sensitivity decreased to half the initial value after one month, which was followed by the loss in stability of the signal. Also worth mentioning was the selectivity toward penicillin of the EIS-NT-penicillinase biosensor. In the course of the experiments, highly concentrated glucose (50 mM) and polymix buffer solutions were alternately added with the penicillin solutions, but no signal changes were noted with either glucose or polymix solutions.

A possible explanation for the enhanced sensor performance for penicillin detection caused by SWNTs may be related to the architecture employed for the film fabrication, which alters strongly the LbL film morphology and affects the electrochemical properties of the sensors. The intimate contact between dendrimers and a dense network of SWNTs forms stable multilayers with highly interconnected nanotubes among them (see Fig. S1 in the supplementary material). As a result, the film porosity is increased, permitting easier penetration of  $\text{H}^+$  ions from the

enzymatic reaction onto the Ta<sub>2</sub>O<sub>5</sub> surface. One can suppose that the PAMAM/SWNT film acts as a suitable porous nanomembrane with a larger active surface area, which allows both a better distribution and attachment of a higher amount of enzyme immobilized on its surface. Simultaneously, buffer molecules from the analyte are hindered to “compensate” the free H<sup>+</sup>-ions inside the porous nanomembrane due to the enzymatic reaction.

The large amount of immobilized penicillinase was confirmed by FESEM images, upon comparing a bare EIS and an EIS-NT sensor, both containing penicillinase atop their surfaces (see Fig. S3 in the supplementary material). The images have the same magnification (10.0 K). As expected, the EIS-NT sensor exhibited a larger, homogeneously distributed amount of immobilized enzyme. This difference demonstrates that one can correlate the effects on the sensing properties of EIS sensors directly with the LbL-SWNT film architecture. Significantly, the combination of carbon nanotubes and dendrimers led to a unique nanostructure, quite suitable for enzyme immobilization, indicating that this approach can be applied to enzymatic-based sensors.

#### 4. Conclusions

We have shown that the incorporation of a nanostructured dendrimer/carbon nanotube LbL film on an EIS structure enhanced the sensitive characteristics for detecting penicillin G, with improved sensitivity, stability and response time. The latter was due to the nanoporous structure with larger active surface area exhibited by the PAMAM/SWNT films, which allowed a better distribution and adsorption of penicillinase, and a faster H<sup>+</sup>-ion penetration through the film. In addition, the concept demonstrated here opens the way for applying CNTs nanostructured films in new biosensor prototypes using field-effect devices.

#### Acknowledgments

The authors thank M. Bäcker and H.-P. Bochem for the AFM and FESEM images, respectively. Financial support from CAPES (Brazil) is gratefully acknowledged.

#### Appendix A. Supplementary data

Supplementary data associated with this article can be found, in the online version, at doi:10.1016/j.bios.2009.07.007.

#### References

- Abouzar, M.H., Poghossian, A., Razavi, A., Besmehn, A., Bijmens, N., Williams, O.A., Haenen, K., Wagner, P., Schöning, M.J., 2008. *Phys. Status Solid. A* 205 (9), 2141–2145.
- Abouzar, M.H., Poghossian, A., Razavi, A., Williams, O.A., Bijmens, N., Wagner, P., Schöning, M.J., 2009. *Biosens. Bioelectron.* 24 (5), 1298–1304.
- Allen, B.L., Kichambare, P.D., Star, A., 2007. *Adv. Mater.* 19 (11), 1439–1451.
- Ariga, K., Hill, J.P., Ji, Q.M., 2007. *Phys. Chem. Chem. Phys.* 9 (19), 2319–2340.
- Balasubramanian, K., Burghard, M., 2006. *Anal. Bioanal. Chem.* 385 (3), 452–468.
- Byon, H.R., Choi, H.C., 2006. *J. Am. Chem. Soc.* 128 (7), 2188–2189.
- Gun, J., Schöning, M.J., Abouzar, M.H., Poghossian, A., Katz, E., 2008. *Electroanalysis* 20 (16), 1748–1753.
- Hammond, P.T., 2004. *Adv. Mater.* 16 (15), 1271–1293.
- Jiang, C., Markutsya, S., Pirus, Y., Tsukruk, V., 2004. *Nat. Mater.* 3 (10), 721–728.
- Kim, S.N., Rusling, J.F., Papadimitrakopoulos, F., 2007. *Adv. Mater.* 19 (20), 3214–3228.
- Lee, S.-R., Rahman, M.M., Sawada, K., Ishida, M., 2009. *Biosens. Bioelectron.* 24 (7), 1877–1882.
- Lutkenhaus, J.L., Hammond, P.T., 2007. *Soft Matter* 3 (7), 804–816.
- Olek, M., Ostrander, J., Jurga, S., Mohwald, H., Kotov, N., Kempa, K., Giersig, M., 2004. *Nano Lett.* 4 (10), 1889–1895.
- Patolsky, F., Timko, B.P., Zheng, G.F., Lieber, C.M., 2007. *MRS Bull.* 32 (2), 142–149.
- Poghossian, A., Abouzar, M.H., Sakkari, M., Kassab, T., Han, Y., Ingebrandt, S., Offenhäusser, A., Schöning, M.J., 2006. *Sens. Actuators B* 118 (1–2), 163–170.
- Poghossian, A., Abouzar, M.H., Amberger, F., Mayer, D., Han, Y., Ingebrandt, S., Offenhäusser, A., Schöning, M.J., 2007a. *Biosens. Bioelectron.* 22 (9–10), 2100–2107.
- Poghossian, A., Ingebrandt, S., Abouzar, M.H., Schöning, M.J., 2007b. *Appl. Phys. A* 87 (3), 517–524.
- Schöning, M.J., Poghossian, A., 2006. *Electroanalysis* 18 (19–20), 1893–1900.
- Schöning, M.J., Poghossian, A., 2008. Detection of charged macromolecules by means of field-effect devices (FEDs): possibilities and limitations. In: Zhang, X., Ju, H., Wang, J. (Eds.), *Electrochemical Sensors, Biosensors and Their Biomedical Applications*. Elsevier, Amsterdam (The Netherlands), pp. 187–212, Ch. 7.
- Siqueira Jr., J.R., Gasparotto, L.H.S., Crespilho, F.N., Carvalho, A.J.F., Zucolotto, V., Oliveira Jr., O.N., 2006. *J. Phys. Chem. B* 110 (45), 22690–22694.
- Siqueira Jr., J.R., Crespilho, F.N., Zucolotto, V., Oliveira Jr., O.N., 2007. *Electrochem. Commun.* 9 (11), 2676–2680.
- Siqueira Jr., J.R., Gasparotto, L.H.S., Oliveira Jr., O.N., Zucolotto, V., 2008. *J. Phys. Chem. C* 112 (24), 9050–9055.
- Siqueira Jr., J.R., Abouzar, M.H., Bäcker, M., Zucolotto, V., Poghossian, A., Oliveira Jr., O.N., Schöning, M.J., 2009. *Phys. Status Solid. A* 206 (3), 462–467.
- Stred'anský, M., Pizzariello, A., Stred'anská, S., Miertuš, S., 2000. *Anal. Chim. Acta* 415 (1–2), 151–157.
- Tang, Z., Wang, Y., Podsiadlo, P., Kotov, N.A., 2006. *Adv. Mater.* 18 (24), 3203–3224.
- Xue, W., Liu, Y., Cui, T., 2006. *Appl. Phys. Lett.* 89 (16), 163512–163513.
- Yang, M., Yang, Y., Yang, H., Shen, G., Yu, R., 2006. *Biomaterials* 27 (2), 246–255.
- Zucolotto, V., Pinto, A.P.A., Tumolo, T., Moraes, M.L., Baptista, M.S., Riul, A., Araujo, A.P.U., Oliveira Jr., O.N., 2006. *Biosens. Bioelectron.* 21 (7), 1320–1326.
- Zucolotto, V., Daghestanli, K.R.P., Hayasaka, C.O., Riul, A., Ciancaglini, P., Oliveira Jr., O.N., 2007. *Anal. Chem.* 79 (5), 2163–2167.